

Allotropic conversion of carbon-related films by using energy beams

© H. Naramoto, Xiaodong Zhu, Yonghua Xu, K. Narumi, J. Vacik, S. Yamamoto*, K. Miyashita**

Advanced Science Research Center, Japan Atomic Energy Research Institute,
1233 Watanuki, Takasaki, Gunma 370-1292, Japan

*Department of Materials Development, Japan Atomic Energy Research Institute,
1233 Watanuki, Takasaki, Gunma 370-1292 Japan

**Gunma Pref. Industrial Technology Res. Lab.;
190 Toriba Maebashi, Gunma 371-0845, Japan

Energy beams such as ion and laser beams were employed to convert carbon allotropes into another ones at the specified position because these energy sources can be controlled precisely in time and space. The ion beam deposition technique employing mass-separated ions was effective to study the nucleation process by changing several growth parameters (ion species, incident energies and substrate temperatures). Immersed nano-sized diamonds were found in sp^3 rich amorphous film prepared with 100 eV $^{12}\text{C}^+$ ions at room temperature. Surrounding these nano-diamonds, the regularly arrayed small bumps, "petals", were formed around the periphery of bald circles when cooling down. The Ar ion laser illumination is effective to design the array of high luminescent points on a C_{60} film by careful control of laser power, and a combination of micro-Raman spectrometer with a piezo-scanning system provides us a tool for 2-dimensional processing of photo-sensitive materials. The simultaneous bombardment during the C_{60} evaporation results in the interesting pattern formation specific for the simultaneous treatment. The dependence of surface nano-scale pattern on the ion energy and the substrate temperatures provides us a new tool to design the nano-scale functional materials. As an extreme, the appearance of hexagonal diamonds was detected with the disordered carbon and graphite under the condition of high ratio between the Ne ion beam and the C_{60} thermal beam.

Carbon atoms condense in various kinds of chemically bonded forms, and they exhibit the remarkably excellent and characteristic properties depending on the bonding nature, which has induced the broad research and applications not only in the materials science but also in other scientific fields. Because of these potential applications the much attention has been paid how to convert the carbon allotropes into another in a controlled manner. As well recognized, the role of catalytic materials is important to convert C_{60} into nano-tubes and/or diamond in a more moderate way. The co-evaporation of Ni with C_{60} at high temperature results in the self-organized structure through the competitive process between the segregation of each component and the possible chelate formation [1]. In this case, the polymerization of C_{60} and graphitization were also observed. The careful studies have been carried out to elucidate the catalytic behavior depending on the cluster size from the electronic and atomistic points of view [2–4]. These chemical processes are attractive because they are not so destructive and energy-saving, but if one wants to intend the materials-design with the specified function it is inevitable to rely on other physical process such as the directional energy beams.

The careful beam tuning in the energy, the energy density and the beam size is also useful to change the bonding nature into another one at the specified area, and this will become the special advantage in the materials design in a small scale. For example, in the super-saturated mixture between transition metals and C_{60} , they form the uniform mixture or the layered structure without mixing in the low temperature deposition. In this situation, C_{60} molecules will play a role of inert gas atoms such as Ar atoms so as to keep Ni clusters separated but, if the mixture is exposed to the intense electronic excitation of energetic ions, C_{60}

molecules can be converted into amorphous carbon, and the segregation of Ni atoms can be facilitated [5]. The energy beams cannot be used to break up but also to push the limited number of atoms into another quasi-stable phase, which is characteristic in ion-beam-assisted deposition (IBAD) technique [6–8]. As one of the extremes in IBAD techniques ion-beam deposition (IBD) technique has been employed to study about the nucleation process of diamonds without the influence of sputtering [9], and it was shown that the ion species and the incident energy are the dominant parameters for amorphous carbon films with higher sp^3 bonding fraction [10].

Here in this report, the attention will be focused on the appearance of nano-scale topological features combined with the dynamical conversion of C_{60} molecules into another carbon allotropes as a function of the beam energy, the substrate temperature and the relative amount of ion beam to the C_{60} molecule beam. As typical examples are illustrated the topographic features obtained in IBD and laser processing experiment for a comparison. The results obtained in this IBAD experiment imply that if the additional parameter is introduced, such as the incident beam direction, the materials design will become more facilitated.

1. Experimental details

The IBD was performed by employing an accelerator-decelerator system under the ultra high vacuum and $^{12}\text{C}^+$ ions were incident to Si(111) and Ir(100)/MgO(100) single-crystalline substrate [11]. The typical ion beam parameters are 50–200 eV in the energy, and around $1\mu\text{A}$ in the beam current after removing energetic neutral species. The crystal quality of Ir(100)/MgO(100) substrate was improved

after the optimization of substrate temperature and the X-ray diffraction analysis and Rutherford Back Scattering (RBS)/channeling analysis show the crystal perfection to be comparable to Si wafer [12].

The IBAD was made by developing a specially designed chamber as described elsewhere [13]. In this chamber three different sources (C_{60} , Ne ions and transition metals) are available. When evaporating C_{60} molecules energetic Ne^+ ions were introduced in the energy range up to 5 keV. The Ne^+ ion beam is obliquely incident with 60° relative to the surface normal, and the sputtering effect should be considered if one uses ions with high Z element. The chamber can be evacuated up to $1.2 \cdot 10^{-6}$ Pa, and in the IBAD experiment the vacuum was maintained less than $5 \cdot 10^{-5}$ Pa. The vapor pressure of C_{60} was maintained to be constant by controlling the temperature of a Knudsen cell at $370^\circ C$, and simultaneously growing C_{60} film was bombarded with Ne^+ ions in the energy range from 0 to 5 keV. The total amount of incident ions was counted by digitizing the incident current on a target holder. The sub-micron sized structure after IBAD treatment was analyzed with two kinds of micro-Raman spectrometers by using an Ar ion laser (Renishaw 2000 with several micron laser spot and a Nano-finder from Tokyo Instrument with the sub-micron size spot for the 514 nm line). The nano-scale surface characterization was made with an atomic force microscope (JSPM-4200). The optical absorption spectroscopy in visible and ultraviolet region was used to assess the optical band gap of the deposited films.

2. Results and discussions

In the IBAD experiment one can realize the more sophisticated condition for the nucleation study of diamond for example. The $^{12}CH_x^+$ ($x = 0-4$) ions with different energies (50–200 eV) are incident on two kinds of substrates (Si(111) and Ir(100)/MgO(100)) at different temperatures (room temperature — $700^\circ C$). In any cases the amorphous graphite films were formed with the sp^3 main features but the highest sp^3 fraction (80%) was obtained under the following condition: 100 eV $^{12}C^+$ ions at room temperature on either substrate. It is surprising that the simultaneous incident with hydrogen atoms as in the experiment using $^{12}CH_x^+$ is effective for the high formation rate of sp^3 bonding. Fig. 1 illustrates a set of photographs from the IBAD carbon films on Ir(100)/MgO(100), synthesized under the highest sp^3 fraction condition. Fig. 1,*a* is an optical micrograph with the 500 times multiplication roughly, and it was taken when the film was heated up to $400^\circ C$ under the He flowing gas. In this photo one can see many bright circles associated with small dots, "flower patterns". The main part of this pattern was formed when heating but the regularly arranged dots were found when cooling down. This phenomena was not observed in the IBAD films on Si(111) substrates. The IBAD films on Si are resistive up to $600^\circ C$ by heating, and after $700^\circ C$ they started to change

into graphite judging from Raman analysis. On the contrary, the IBAD films on Ir/MgO are not resistive for heating, and after heating at $400^\circ C$ a part of the film started to be taken off. But the remaining part has the sp^3 nature. Each "flower" seems to be formed at the crystal imperfections of the substrate crystal with a small dot at the center. The similar flower patterns were also observed on Ir(110)/MgO(110) with the (110) symmetry. Fig. 1,*b* illustrated the atomic force microscope (AFM) analysis on a single flower among the many flower patterns in the same film. The regularly arranged dots around "flowers" can be observed clearly, and the elemental analysis on this evidenced that the dots are a kind of blister with small loss of carbon component. Through the above-decribed information it is reasonable to conclude that the regularly arranged dots with the fractal nature are formed through the deformation instability when the fast temperature change in the cooling process. The nano-dot at the center (roughly 300 nm in diameter) is also interesting, and the micro-Raman analysis with the sub-micron laser spot was performed. The study gives us a clear evidence of finding out immersed nano-diamonds in the dominant sp^3 amorphous carbon film.

The illumination of C_{60} films on Si with an Ar ion laser resulted in interesting features (not shown for the simplicity). By a careful tuning of the energy density it has become possible to prepare the high luminescent points with the sub-micron size through the polymerization of C_{60} films. The array of the high luminescent points can be designed easily by using a micro-Raman spectrometer combined with the AFM stage. The illumination with the high energy density or with the longer exposure simply induced the graphitization. Further studies are scheduled to know the detailed of polymerization by changing the wavelength of lasers.

Relating to the carbon allotrope conversion, the strong attention was paid for the competitive process between the C_{60} evaporation and the ion bombardment (IBAD). The main parameters in the IBAD experiment are the Ne^+ ion energies (0–5 keV), the substrate temperatures (room temperature — $800^\circ C$) and the relative ratio between the Ne^+ ion beam intensity and the C_{60} molecular beam intensity. The Ne^+ ion energy increase improved the quality of the C_{60} film on Si(111) in the sense of Raman spectrum in the low energy region up to 500 eV but in the medium energy region from 600 to 1000 eV the amorphous carbon films with the asymmetric feature in Raman spectra were formed. And in the high energy region from 1600 to 4800 eV, the clear graphitization was detected with the more efficient deposition rate of carbon atoms in comparison with the deposition in the medium temperature region. The corresponding analysis on the surface morphology and the optical band gap was carried out by employing AFM observation and optical absorption measurement, respectively. The surface analysis revealed the mound-like structure in the broad energy range from 1000 to 5000 eV but the details are different (not shown

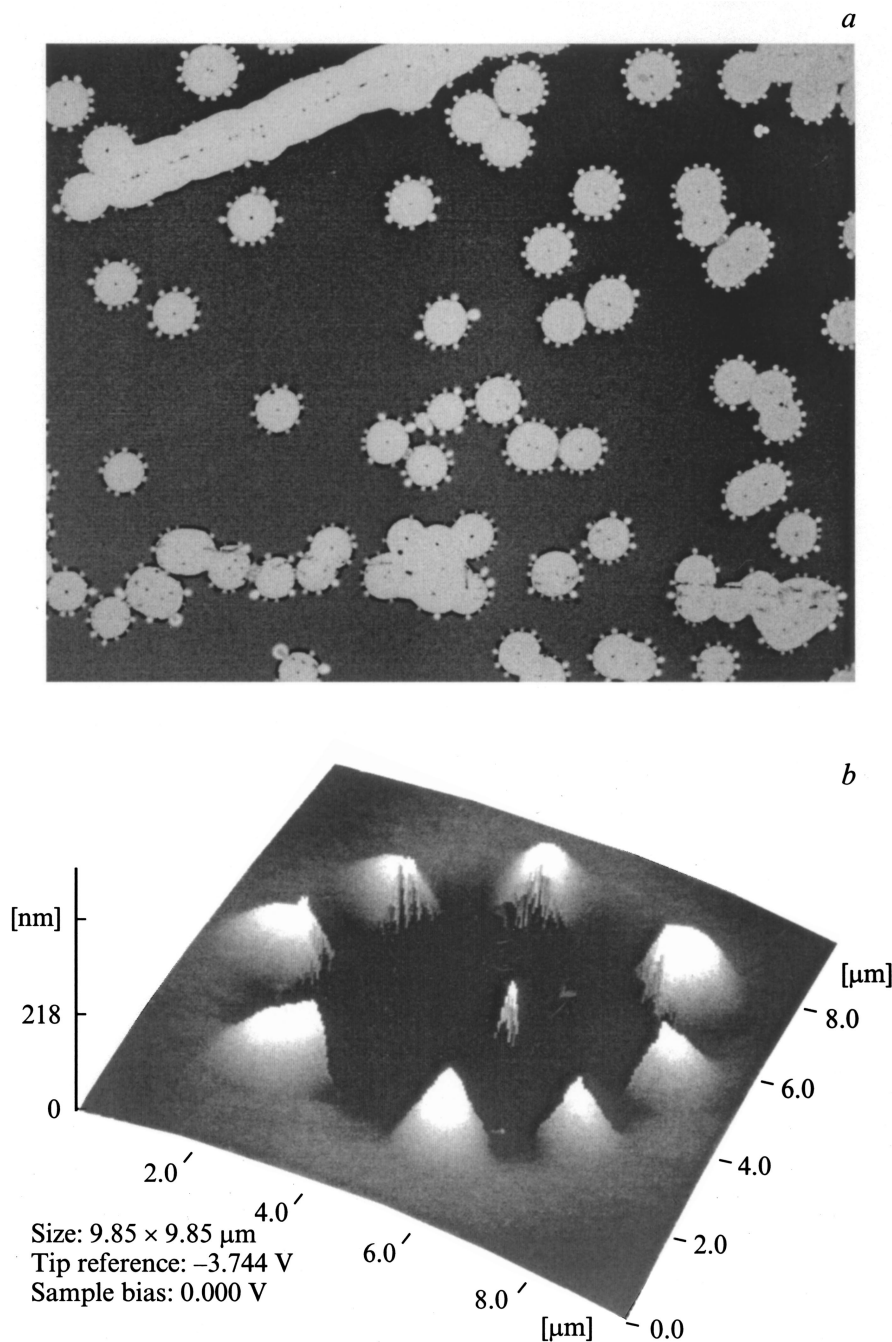


Figure 1. Surface characterization of sp^3 -rich DLC on IR(100)/MgO(100) heated at 700°C under flowing He gas. *a* — optical micrograph ($\times 500$). Many "flower" patterns can be seen. *b* — AFM image of a "flower" pattern with a nano-diamond at the center. Regularly arranged small "petals" are formed through the instability in the fast stress-relaxation process.

for simplicity). The diameter and the height in the mound-like structure are larger for the high energy treated films, and through the correlation analysis the change of diameter seems to be non-linear as a function of the Ne^+ ion energy. The optical band gaps evaluated shows the maximum around 1600 eV in this study (around 1.7 eV), and in the higher energy region it goes down to the value corresponding to the graphite. In the next, the temperature dependent topological features were analyzed with AFM in the temperature range

from 200 to 700°C . Fig. 2 is a set of AFM images from the IBAD films prepared at different temperatures. In the low temperature region one can recognize the mound-like structure with the a few 10's nanometer, the same as in the ion energy dependence study, and with coming close to 550°C some transition feature with the vague image is observed. Further increase of substrate temperature up to 700°C induces the dramatic change into the ripple-like structure. This arrangement of ripples is correlated to the

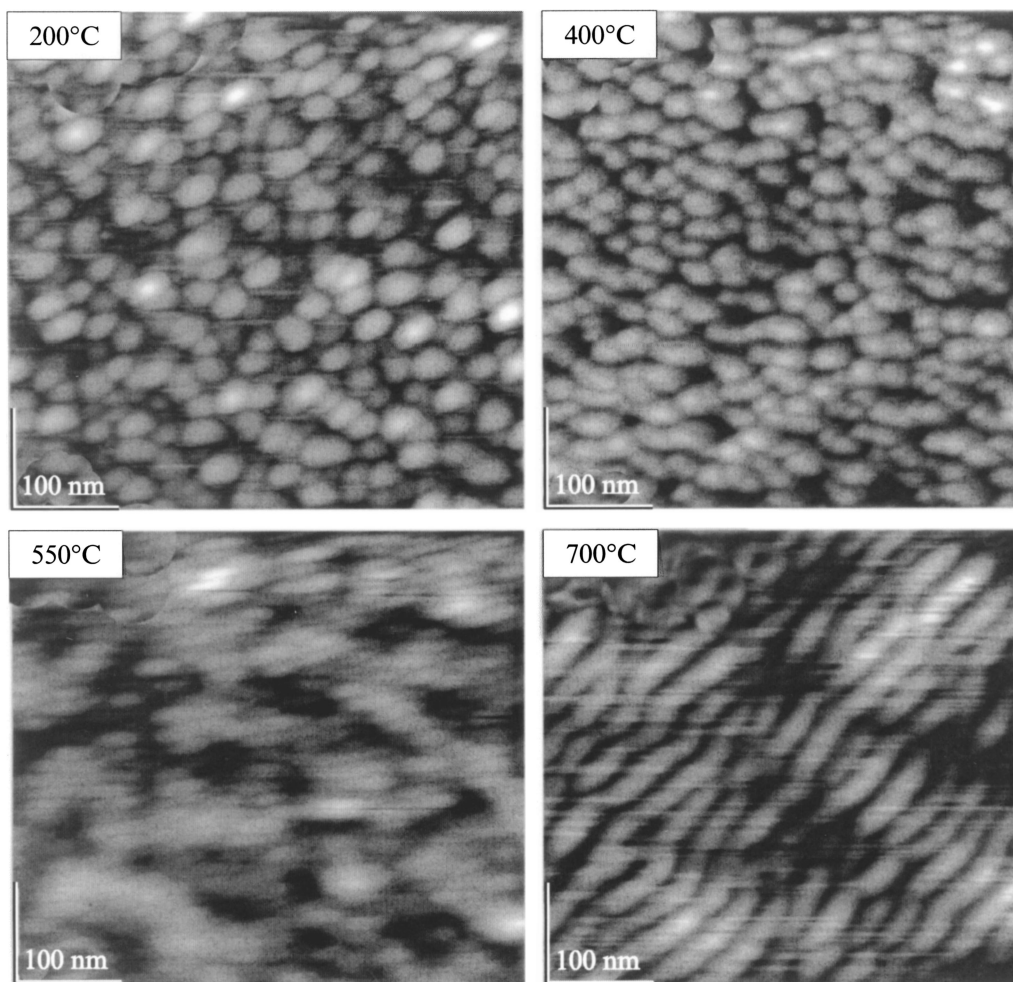


Figure 2. AFM characterization of carbon films as a function of the deposition temperature. 200°C (top left), 400°C (top right), 550°C (bottom left) and 700°C (bottom right). The Ne^+ ion energy is fixed at 1.5 keV.

step structure in the Si substrate after heat treatment. In the IBD experiment with the less ion beam intensity, the self-organized dot array of SiC was observed along the single step of a Si substrate was observed at the same temperature range, but in the present case the resultant intensity of carbon source after breaking C_{60} molecules is dominant. The present result with an additional Raman analysis shows us that the high temperature deposition induces the graphite ripple structure with some periodic nature. This feature can be useful the material design employing the self-organization process.

The further study was made by changing the relative intensity between the Ne^+ ion beam and the C_{60} molecular beam. The decrease of the relative intensity resulted in the graphitic feature in the Raman spectrum but in the other case there appeared the Raman lines relating to hexagonal diamonds with the rippled surface structure. Fig. 3 shows the typical Raman spectrum found in the sample prepared at the high ratio between Ne^+ beam intensity and C_{60} beam intensity (1.5 keV Ne^+ , 700°C). Different from the previous samples described above, the Raman lines are

sharp, and one can easily recognize the co-existence between hexagonal diamonds, and disordered carbon and graphite. The Raman lines at 1157, 1199 and 1326 cm^{-1} can be attributed to the hexagonal diamonds [14–17], and the others at 1584 and 1604 cm^{-1} to the disordered carbon and graphite, respectively. The X-ray diffraction analysis mainly manifests the features of hexagonal diamond with 2H-, 8H-, 12H-, and 20H-polytypes. The size of the hexagonal diamonds is estimated as the order of 30 nm based on the X-ray diffraction line. Under the present ion beam condition, a great deal of thermal and displacement spikes can be created along the ion trajectories. The rapid quenching of these spikes on growing surface results in the preferential damage of graphite because diamond is more resistive for the displacement than graphite. However, this effect takes place depending strongly on the substrate temperature. Only in an intermediate temperature range, the probability for relaxation into diamond site is sufficiently large. Otherwise, graphite becomes again the stable phase. In the present work, the temperature dependence of nanocrystalline diamond growth is in a good agreement with

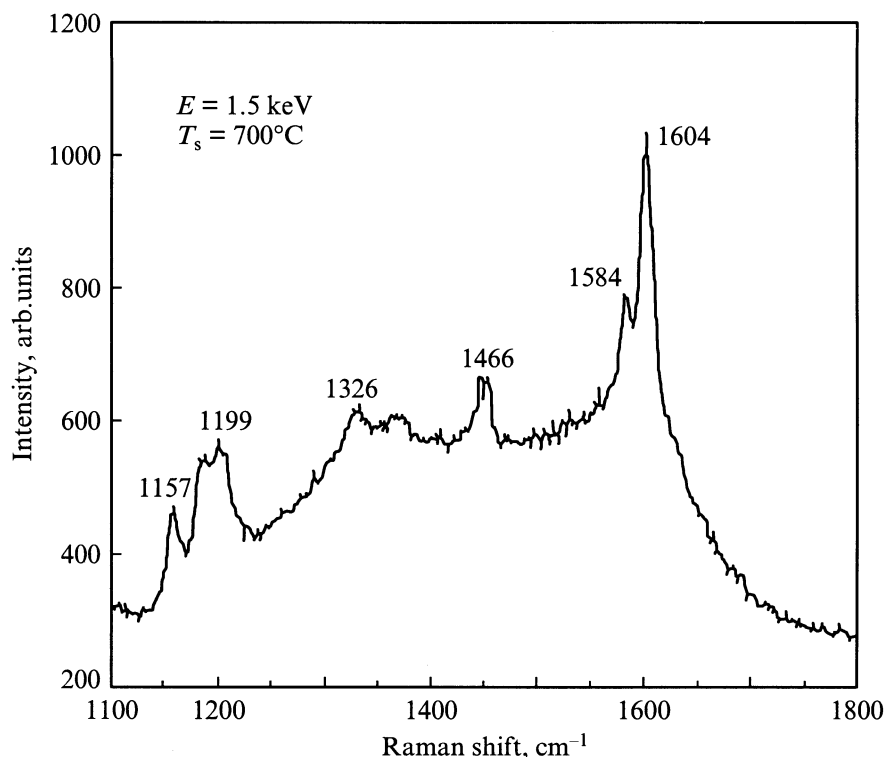


Figure 3. Raman spectrum in a carbon film prepared with high ratio between the Ne^+ ion beam and the C_{60} molecular beam (1.5 keV Ne^+ , 700°C).

this argument. Our experiment clearly demonstrates the substrate temperature as high as 700°C is necessary to form hexagonal diamond. It is said that the irradiation-induced effect produces hexagonal diamonds more easily than the cubic ones due to the similar effect to "shock-compression".

3. Summary and conclusions

The systematic IBD experiment revealed the nano-diamonds immersed in the dominant sp^3 amorphous carbon films. C and Ir are immiscible but the C-implantation together with the defect introduction can favor the supersaturated carbon atoms in the subsurface region. The heat treatment can help the further growth from the nucleated embryos. It is interesting to control the nucleation sites with the help of ion beam technique as a further study.

The array of high luminescent points is realized through the proper treatment of the C_{60} film with a Ar ion laser. The present observation can be closely related to the polymerization of the C_{60} film, and the further study is required to know the details by changing the wavelength of illuminating laser.

In the IBD experiment, the systematic studies, by changing the ion energies and substrate temperatures, provide us the interesting features of nano-pattern formation. The patterns observed can be formed through the dynamical process between the sputtering and the deposition. In the deposition with the intense Ne^+ ion current, hexagonal

diamonds with nano-size were prepared from the C_{60} vapor with the simultaneous bombardment of 1.5 keV Ne^+ ions at the proper temperature of 700°C. The Raman features are consistent with the Raman modes predicted by the calculations or by experimental observation. It is also found that graphite co-exists in the sample. Due to ion sputtering effect, the surface of the film exhibits regular periodical ripple patterns.

The authors are thankful for the incessant support by the people in the Advanced Science Research Center, especially Prof. H. Yasuoka. Several authors, Y.X., J.V., V.L., are indebted to JAERI Research Fellowship systems. X.Z. is also thankful for the STA exchange program.

References

- [1] J. Vacik, H. Naramoto, K. Narumi, S. Yamamoto, K. Miyashita. *J. Chem. Phys.* **114**, 9115 (2001).
- [2] C. Cepek, A. Goldoni, S. Modesti. *Phys. Rev.* **B53**, 7466 (1996).
- [3] A. Andriotis. *Phys. Rev.* **B60**, 4521 (1999).
- [4] F. Banhart, J.-C. Charlier, P.M. Ajayan. *Phys. Rev. Lett.* **84**, 686 (2000).
- [5] H. Naramoto, J. Vacik, S. Yamamoto, K. Narumi, Y. Xu. *JAERI-Review* **2000-024**, 157 (2000).
- [6] H. Hirai, M. Terauchi, M. Tanaka, K. Kondo. *Phys. Rev.* **B60**, 6357 (1999).
- [7] E. Grossman, G.D. Lempert, J. Kulik, D. Marton, J.W. Rabalais, Y. Lifshitz. *Appl. Phys. Lett.* **68**, 1214 (1996).

- [8] V.I. Merkulov, D.H. Lowndes, G.E. Jellison Jr., A.A. Poretzky, D.B. Geohegen. *Appl. Phys. Lett.* **73**, 2591 (1998).
- [9] H. Ohno, J.A. van den Berg, S. Nagai, D.G. Armour. *Nucl. Instr. Meth.* **B148**, 673 (1999).
- [10] Z. Tang, Z.J. Zhang, K. Narumi, Y. Xu, H. Naramoto, S. Nagai. *J. Appl. Phys.* **89**, 1959 (2001).
- [11] H. Naramoto, Y.H. Xu, X.D. Zhu, K. Narumi, J. Vacik, S. Yamamoto, K. Miyashita. *Proc. Mat. Res. Soc.* **647**, O-5 18-1 (2001).
- [12] H. Naramoto, S. Yamamoto, K. Narumi. *Nucl. Instr. Meth.* **B161–163**, 534 (2000).
- [13] X.D. Zhu, Y.H. Xu, H. Naramoto, K. Narumi. Privat communication.
- [14] F.P. Bundy, J.S. Kasper. *J. Chem. Phys.* **46**, 3437 (1967).
- [15] T. Yagi, W. Utsumi, M. Yamakata, T. Kikegawa, O. Shimomura. *Phys. Rev.* **B46**, 6031 (1992).
- [16] M. Nishishitani-Gamo, T. Tachibana, K. Kobayashi, I. Sakaguchi, K.P. Loh, K. Yamamoto, T. Ando. *Dia. and Related Mater.* **7**, 783 (1998).
- [17] B.R. Wu, J. Xu. *Phys. Rev.* **B57**, 13355 (1998).